

## Automated X-ray Inspection Method for Fillet-less Mounted Chip Components

Atsushi Teramoto<sup>\*a</sup>, Member  
Takayuki Murakoshi<sup>\*</sup>, Non Member  
Masatoshi Tsuzaka<sup>\*\*</sup>, Non Member  
Hiroshi Fujita<sup>\*\*\*</sup>, Non Member

Chip components mounted on the printed circuit board are rapidly being miniaturized. Furthermore, the fillet-less chip soldering technique, which does not use a solder fillet, is widely used in portable products such as mobile phones. However, there is no method to inspect the soldering of fillet-less chip mounting. In this paper, we propose an automated X-ray inspection technique for fillet-less chip mounting. It extracts three inspection parameters from the X-ray image. In the experiments, we evaluate the repeatability and inspecting ability of the technique and confirm that sufficient information for failure detection is obtained. An automated X-ray inspection system using this technique is now in operation at some factories, so in conclusion our automated method would be useful in practice. © 2007 Institute of Electrical Engineers of Japan. Published by John Wiley & Sons, Inc.

**Keywords:** X-ray, fillet-less, soldering, automated inspection

*Received 28 September 2006; Revised 6 November 2006*

### 1. Introduction

Owing to the strong demand for compact and lightweight electronic consumer products, engineers have integrated small and high-density electrical components on printed circuit boards. In particular, remarkable miniaturizations of passive components such as the chip resistors and capacitors have been achieved. Tiny chip components with dimensions of  $0.6 \times 0.3 \text{ mm}^2$  and  $0.4 \times 0.2 \text{ mm}^2$  are widely adopted in mobile phones [1]. Furthermore, some products employ the fillet-less mounting, which does not have a solder fillet at both sides of the chip components, to increase the mount density. In this paper, we focus on the inspection techniques for the fillet-less chip mounted board.

Historically, the soldering of chip components was inspected by optical techniques by evaluating the shape of the solder fillet [2].

However, the optical technique cannot be adapted to fillet-less mounting because the junction is formed between an electrode on the under side of a component and a printed circuit board. In order to inspect the soldering that is hidden from view, X-ray inspection is the most effective method [3]. However, automated inspection technique for fillet-less soldering has not been proposed. In this paper, we propose an automated X-ray inspection method for fillet-less mounted chip components.

### 2. Image Characteristics of Fillet-less Chip Mounting

Because the gray level of X-ray image corresponds to the solder thickness, actual solder thickness is obtained by comparing the gray level and the thickness of solder standard step-wedge, which is installed in the inspection system. When we capture the X-ray image of the chip resistor, only the solder shape is obtained because the chip resistor barely absorbs X-rays. On the other hand,

<sup>a</sup> Correspondence to: Atsushi Teramoto.

E-mail: [tera@oe.nagoya-denki.co.jp](mailto:tera@oe.nagoya-denki.co.jp)

\* Nagoya Electric Works Company, Limited, 550 Katori, Tado-cho, Kuwana 511-0102, Japan

\*\* Department of Radiological Technology, Nagoya University, 1-1-20 Daiko-Minami, Higashi-ku, Nagoya 461-8673, Japan

\*\*\* Department of Intelligent Image Information, Graduate School of Medicine, Gifu University, 1-1 Yanagido, Gifu 501-1194, Japan

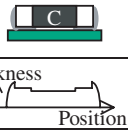
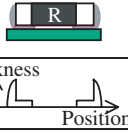
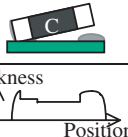
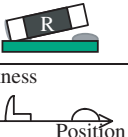
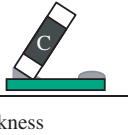
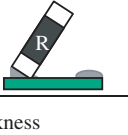
	Chip Capacitor	Chip Resistor
(a) Good model		
(b) Defective model 1		
(c) Defective model 2		

Fig. 1 The appearances and thickness profile curves in the X-ray image for two fillet-less mounted chip components

the solder and chip shape overlap in the chip capacitor's X-ray image because there are several metal plates inside it. Figure 1 defines the appearance and thickness profile curve in the X-ray image that have to be inspected by the proposed method. We denote the characteristics of a good and defective sample as follows.

**2.1. Good model** Figure 1(a) shows the appearance and thickness profile curve of good soldering. In the fillet-less mounting, some solder goes to the end side of the chip components, while the rest goes to the rear of the electrode. The solder under the electrode contributes to the solder joint.

**2.2. Defective model 1** When one side of a component is lifted slightly, the appearance and thickness profile curve appear as shown in Fig. 1(b). The solder thickness under the electrode of the lifted side becomes larger than that in a good sample. As for the chip resistor, the difference in the shape of the thickness profile between the good and defective sample becomes larger.

**2.3. Defective model 2** When the lift angle of the components becomes larger than that in defective model 1, the appearance and thickness profile curve appear as shown in Fig. 1(c). In the chip capacitor, the component length appears to shrink in the profile. The shape of the resistor is the same as that in defective model 1.

On the other hand, we do not consider the following defects in this paper because these are easily detectable by the conventional optical inspection technique: wrong amount of solder supply, bridge, missing parts, and improper arrangement of parts.

### 3. Inspection Method

To inspect the fillet-less mounted chip components, we introduced the following three characteristics.

(1) Chip lift angle derived from thickness of the electrode:  $\theta_1$

The chip lift angle  $\theta_1$  is calculated by using the difference of the solder thickness on both sides of the electrode, as shown in Fig. 2. If  $\theta_1$  exceeds the threshold, the chip is judged to be defective.

$$\theta_1 = \tan^{-1} \frac{D}{L} \quad (1)$$

Here,  $D$  is the difference of the solder thickness on both sides of the electrode and  $L$  is the distance between both electrodes.

(2) Components lift angle derived from its length:  $\theta_2$

It is effective to measure the lengths of the components from an X-ray image when their lift angles become large. Assuming the actual chip length as  $L_1$  and measured chip length as  $L_2$ , as shown in Fig. 3, the chip lift angle  $\theta_2$  is defined as follows.

$$\theta_2 = \cos^{-1} \frac{L_2}{L_1} \quad (2)$$

where  $L_1$  can be obtained from the specification of the chip components and  $L_2$  is calculated as the distance between both edges of the chip components in the X-ray image. This parameter is an effective technique only for the chip capacitor where component shapes exist in the X-ray image.

(3) Normalized correlation of solder shape on electrode: SC [4]

The solder shape of the electrode changes because of the lift of the components. To evaluate the solder shape, the cross correlation of the previously acquired model image and the captured chip image is calculated

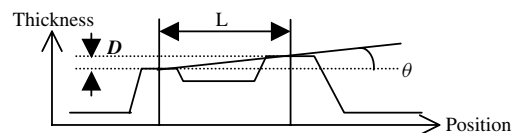


Fig. 2 Difference of thickness at electrode observed in X-ray profile curve

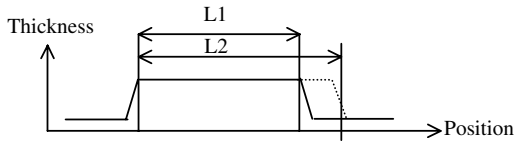


Fig. 3 Change of length due to the component lift in X-ray profile curves

as follows, and it is assumed to be the shape score,  $SC$ .

$$SC = \frac{N \sum_x \sum_y I(x, y) \cdot M(x, y) - \sum_x \sum_y I(x, y)}{\sqrt{A \cdot B}} \quad (3)$$

$$A = N \sum_x \sum_y I(x, y)^2 - \left( \sum_x \sum_y I(x, y) \right)^2$$

$$B = N \sum_x \sum_y M(x, y)^2 - \left( \sum_x \sum_y M(x, y) \right)^2$$

Here,  $I(x, y)$  is the examined image and  $M(x, y)$  is the model image that is previously captured using a good board.

#### 4. Experiments

We verified the proposed technique using an actual fillet-less chip mounted board. The X-ray profile 2D curves of the chip resistor and capacitor obtained from an X-ray image are shown in Figs 4 and 5. The defective points are marked by arrows in these figures. Table I illustrates the inspection results. In the results of the chip resistor,  $\theta_1$  and  $SC$  of the defective sample is larger and 40% smaller than that of the good sample, respectively. As for the chip capacitor,  $\theta_1$  is effective when the inclined angle of the chip is small, as shown in Fig. 5(b), and  $\theta_2$  is effective when the inclined angle is large, as shown in Fig. 5(c). We also evaluated the repeatability of the inspection. As a result,  $\theta_1$  and  $\theta_2$  were 0.61 degrees and 4.12 degrees, respectively, and  $SC$  was 0.57%. The repeatability of  $SC$  is small when compared to the difference between the good and defective samples in the chip resistor. On the other hand, the repeatabilities of  $\theta_1$  and  $\theta_2$  are larger.

#### 5. Conclusion

We proposed an automated X-ray inspection method for fillet-less chip soldering. Three parameters to detect

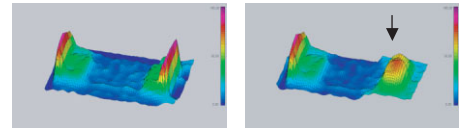


Fig. 4 Shape of the resistor in terms of X-ray profile 2D curves

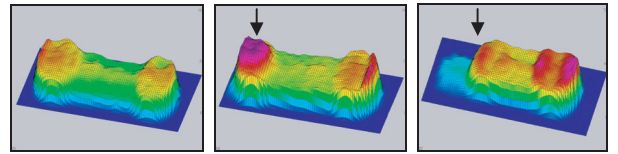


Fig. 5 Shape of capacitor in terms of X-ray profile 2D curves

Table I. Inspection results in good and defective cases for resistor and capacitor

Sample		$\theta_1$ [°]	$\theta_2$ [°]	$SC$ [%]
Resistor	Good	0.3	—	88.1
	Defective	2.2	—	46.3
Capacitor	Good	0.4	0.0	97.0
	Defective1	2.3	0.0	90.5
	Defective2	0.6	14.8	86.0

the defect of fillet-less chip soldering were introduced. In the experiment, we verified the proposed technique using an actual fillet-less chip mounted board. As a result, these parameters effectively separate good and defective samples. An automated X-ray inspection system using this technique is now in operation at some factories. We will try to improve the inspection ability and repeatability by introducing additional parameters.

#### References

- (1) Hisaki T. *Murata's Technology Paves Way for Ultra-small Capacitors*. 2006; <http://www.murata.com/articles/ta03d1.pdf>.
- (2) Muraoka T, Rice C. Applications of laser system in post-solder inspection equipment. *16th Annual Conference of IEEE Industrial Electronics Society*, Asilomar Conference Center, Pacific Grove, California, 1990; 805–810.
- (3) Teramoto A, Murakoshi T, Horiba I. High speed and high precision solder bump inspection method using X-ray fluoroscopy. *IEEEJ Transaction on Industrial Application* 2005; **125-D(6)**:652–658.
- (4) Rosenfeld A, Kak AC. *Digital Picture Processing*, 2nd Edition. Academic Press: San-Diego, California, 1982; 36–39.